

Synthesis, Physicochemical Analysis, and Characterisation of Periwinkle-Based Chitosan

Ijwo Omirenyi Peter*, B. A Kyenge

Department of Chemistry, Rev. Fr. Moses Orshio Adasu University Makurdi, P. M. B 102119,
Makurdi, KM 4, Gboko Road, Benue State, Makurdi-Nigeria

Abstract: The growing accumulation of shell waste from aquatic food processing presents an environmental challenge and an opportunity for sustainable biopolymer production. This study reports the extraction, physicochemical analysis, and characterisation of chitosan derived from periwinkle shell waste as a locally sourced alternative to conventional crustacean-based chitosan. Chitin was isolated through sequential demineralisation, deproteinisation, and decolourisation, followed by alkaline deacetylation to obtain chitosan. The resulting material was analysed using Fourier Transform Infrared Spectroscopy (FTIR), X-ray Powder Diffraction (XRD), Scanning Electron Microscopy (SEM), and Energy-Dispersive X-ray Spectroscopy (EDX). The extracted chitosan exhibited a high degree of deacetylation (86%), confirming effective conversion from chitin. Physicochemical evaluation revealed low moisture and protein contents (0.5% and 0.4%), indicating good stability, while moderate ash content (5.6%) suggested partial residual mineral presence. FTIR confirmed characteristic functional groups of chitosan, XRD revealed enhanced crystallinity relative to native chitosan, and SEM showed a rough, porous morphology with high surface area. EDX analysis indicated residual calcium from the shell matrix. However, periwinkle shell waste represents a viable and sustainable source of functional chitosan suitable for food, agricultural, environmental, and biomedical applications.

Key points: Periwinkle shell; chitosan; waste valorisation; physicochemical characterisation; biopolymer.

Introduction

The generation of large quantities of waste materials from food processing activities constitutes a growing environmental and public health concern, particularly in developing countries (Hamed et al., 2016). However, such wastes also represent underutilised bioresources that can be valorised into high-value functional materials. Among these, shell wastes from marine and freshwater organisms such as periwinkles and snails classified within molluscs and crustaceans are rich sources of chitin, a naturally occurring biopolymer (Maruthiah & Palavesam, 2017; Rasti et al., 2017; Ramasamy et al., 2017; Hamdi et al., 2017; Ehrlich et al., 2017).

Chitin is recognised as the second most abundant natural polymer after cellulose and is predominantly obtained from marine crustaceans such as shrimps and crabs, as well as from fungal cell walls and insect exoskeletons (Rinaudo, 2006; Chaudhary et al., 2020, 2021). Through a controlled deacetylation process, chitin is converted into chitosan, a more versatile polysaccharide with enhanced solubility and functional properties (Khatri et al., 2020). Chitosan has attracted considerable scientific interest due to its non-toxicity, biodegradability, biocompatibility, and inherent antimicrobial and antioxidative activities (Du et al., 2009).

Periwinkle shells are abundantly available in coastal and riverine communities across Nigeria, where they are commonly discarded as waste following consumption. The successful extraction of chitin from periwinkle shell waste therefore presents a dual advantage: mitigating environmental

pollution while converting an otherwise discarded material into a valuable biopolymer resource. Chitin and its derivative, chitosan, have demonstrated wide-ranging applications in cosmetics, food preservation, surgical sutures, biocomposites, papermaking, and water purification (Farajzadeh et al., 2016; Usman et al., 2016; Al-Manhel et al., 2016; Petrenko et al., 2017). Notably, chitin-derived materials have been explored as fillers in biodegradable polymer composites, with promising potential for biomedical applications such as temporary bone fixation materials due to their biocompatibility.

Beyond its industrial and biomedical applications, chitosan plays a crucial role in agriculture and food systems. Chitosan oligomers interact with cellular components, including DNA, plasma membranes, and cell wall constituents, activating defence-related gene expression in plants (Katiyar et al., 2015; Pichyangkura & Chadchawan, 2015). As a biostimulant, chitosan has been reported to enhance growth, yield, and disease resistance in a wide range of crops, including cereals, fruits, vegetables, and ornamental plants (Pornpienpakdee et al., 2010; Maqbool et al 2010 and Ali et al., 2013).

Given the abundance of periwinkle shell waste in Nigeria and the increasing demand for sustainable, bio-based materials, this study focuses on the extraction of chitin from periwinkle shells, its conversion to chitosan, and the subsequent physicochemical analysis and characterisation of the resulting biopolymer. Such an approach aligns with principles of green chemistry and circular economy, offering a sustainable pathway for waste valorisation while contributing to the growing body of knowledge on alternative, locally sourced chitosan production.

Materials and Methods

Chemical Reagents: All the chemicals and solvents that were used in this study will be of the highest analytical grade or extra purity. Hydrochloric acid (HCl 37% BDH Chemical Limited England), deionised water, Sodium Hydroxide pellets (NaOH 97%BDH Chemical Limited England), Acetone (CH₃COCH₃ 99%BDH Chemical Limited England) were purchased from a recognised chemical company.

Collection and processing of the sample: The periwinkle shells were obtained from Apapa Fish Market, Lagos State. The shells were washed with water, rinsed thoroughly, and dried in the sun for three days. The dry shells were pulverised with a mortar and pestle and sieved using a sieve size of 1.5 mm (1500µm), and the powder was used for chitin extraction.

Chitin and Chitosan Preparation: The production of chitosan involved a series of essential steps, namely: deproteination, demineralisation, depigmentation or decolourization, and deacetylation.

Demineralization: About 500g of the powdered periwinkle shells were measured and placed in a 5000 mL beaker. To the 500 g of powdered periwinkle shells in the beaker, 2500 mL of 2 M HCl (1:5 w/v) solution were added. The mixture was stirred in a shaker at 50 °C for 2 hours to eliminate carbonate and phosphate content, followed by 1 hour of cold shaking at 150 rpm using a shaking device. The resultant insoluble fraction was filtered using Whatman filter paper, rinsed with deionized water until a neutral pH was reached, and dried to a constant weight at 65 °C, then set aside for subsequent use (Sitohy et al., 2022)

Deproteinization: 58g of the demineralised chitin were placed in a 5000 mL beaker, and 870 mL of 11.25 M (45%) sodium hydroxide (NaOH) solution (1:15 w/v) were added. The mixture was stirred and boiled in a water bath set at 80 °C for 5 hours, followed by 1 hour of cold shaking at 150 rpm. The residues were filtered through Whatman filter paper, rinsed with deionized water until a neutral pH was achieved, and then dried at 65 °C to a constant weight (Sitohy et al., 2022)

Decolorization: Decolorization was performed by immersing 58 g of chitin in 870 mL of acetone (15 mL/g) for 2 hours in a water bath at the acetone boiling point (57 °C), followed by 1 hour of cold shaking at 150 rpm to remove oils and pigments. The sample was then filtered and submerged in 870 mL of 95% ethyl alcohol (15 mL/g) for 1 hour in a water bath at the ethanol boiling point (79 °C), followed by 1 hour of cold shaking at 150 rpm for further purification. The chitin was

subsequently filtered and dried at 65 °C to a constant weight for the deacetylation process (Sitohy et al., 2022).

Deacetylation: The deacetylation process, responsible for converting chitin into chitosan, was carried out by treating the obtained chitin (after demineralization and deproteinization) with a concentrated sodium hydroxide solution. The chitin was placed in a 1000 mL beaker, and 750 mL of 50 wt/wt% (12.5 M) NaOH were added and heated at 85 °C for 2 hours and 30 minutes in a water bath, followed by cooling for 30 minutes at room temperature. The mixture was stirred on a magnetic stirrer at 30 °C for 4 hours at 200 rpm, and the resulting chitosan was washed until the pH of the filtrate became neutral upon testing with litmus paper. The product was then filtered using Whatman filter paper and dried to a constant weight at 40 °C, as described by Sitohy et al. (2022).

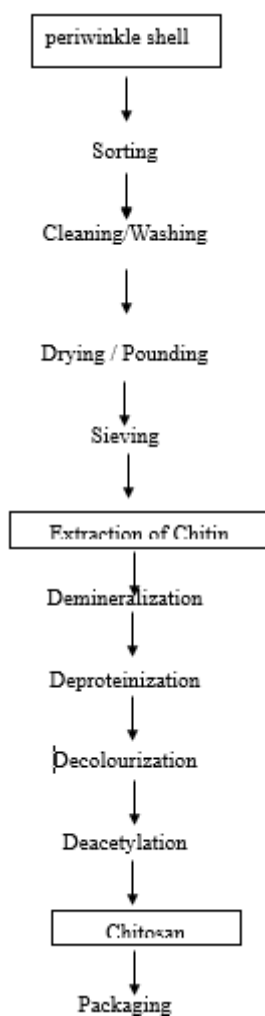


Fig 1. Flow chart of Preparation of Chitosan from Periwinkle Shells

2.4 Determination of the degree of deacetylation of chitosan using FT-IR

The percentage of N-acetyl-glucosamine units is termed the degree of acetylation (DA) and can vary from 50% to 100% (Pellis et al., 2022). The percent acetyl removal or degree of deacetylation is a measure of the extent to which acetyl units are removed from the polymer chain of chitosan (Amitaye et al., 2024; Popuri et al., 2009). The degree of deacetylation (DD%) was determined using an FT-IR spectrophotometer (Bruker, Version 7.5) with a frequency range of 400–4000 cm^{-1} . This was carried out using the equations described by Sánchez-Machado et al. (2024) and Kasaaï (2008).

$$\text{DA}\% = 115 \times (A_{1320} - A_{1420}) \quad (i)$$

Where A_{1320} is absorption of amide III at 1320 cm^{-1} , and A_{1420} is absorption of CH_2 bending at 1420 cm^{-1}

$$DD\% = 100 - DA\% \quad (ii)$$

Here, A_{1320} and A_{1420} correspond to the integral in the band at 1320 cm^{-1} and 1420 cm^{-1} of the spectrum.

Characterisation of the Chitosan

Fourier Transform Infrared Spectroscopy (FTIR)

FTIR spectra for chitosan were captured using an FTIR spectrophotometer (Jasco-Japan 4100) within a frequency range of $400\text{--}4000\text{ cm}^{-1}$. The degree of deacetylation (DD%) for chitosan was determined using the equations provided by Sánchez-Machado et al. (2024) and Kasaai (2008).

$$DA\% = 115 \times (A_{1320} - A_{1420}) \quad (i)$$

Where A_{1320} is absorption of amide III at 1320 cm^{-1} , and A_{1420} is absorption of CH_2 bending at 1420 cm^{-1}

$$DD\% = 100 - DA\% \quad (ii)$$

Here, A_{1320} and A_{1420} corresponds to the integral in the band at 1320 cm^{-1} , and 1420 cm^{-1} of the spectrum.

X-ray powder diffraction (XRD): Chitosan crystallinity was assessed through XRD analysis using a PANalytical X'Pert PRO X-ray machine from the Netherlands. The XRD measurements on the powder samples were conducted with $\text{Cu K}\alpha$ radiation as the X-ray source (45 kV, 30 mA). Scanning of the samples was performed at a rate of 4 min^{-1} and at $25\text{ }^\circ\text{C}$ within the 2θ range of $5\text{--}40^\circ$. The crystalline index (CI%) was determined by calculating the ratio of the crystalline phase to the sum of the crystalline and amorphous phases, using the equation provided by Liu et al. (2012).

Scanning electron microscopy (SEM): SEM (Scanning Electron Microscopy) was employed to investigate the surface morphology of chitosan samples using a High-Resolution Field Emission SEM (Quanta FEG 250, Czechoslovakia). Prior to examination, 10 g of chitosan samples were coated with gold using a sputter coater (Edwards S150ABOC, Edwards, UK) under vacuum conditions to enhance contrast. Images of the sample surfaces were then captured at different magnifications and locations.

Results

Physicochemical Parameters of the Chitosan Extracted from Periwinkle Shells

Chitosan extracted from periwinkle shells demonstrated high quality, with a degree of deacetylation of 86%, low moisture (0.5%) and protein (0.4%) contents, indicating strong stability and suitability for food and biomedical applications. Although the ash content (5.6%) was higher than the ideal range, it remained within values previously reported for periwinkle-derived chitosan and likely reflects partial demineralisation, consistent with residual elemental traces observed in EDX analysis.

Table 1: Physicochemical Parameters of the Chitosan Extracted from Periwinkle Shells

| Parameter | Percentage composition |
|-------------------------|------------------------|
| Degree of Deacetylation | 86% |
| Moisture Content | 0.5% |
| Ash Content | 5.6% |
| Crude Protein Content | 0.4% |

FT-IR spectrum of Periwinkle Chitosan sample (PCHN)

The FTIR spectrum of the periwinkle chitosan (PCHN) (Figure 1) showed key absorption peaks confirming its polysaccharide structure and chitosan identity, including a broad O-H/N-H stretch at 3351.30 cm^{-1} , a C=O stretch at 1785.85 cm^{-1} indicating partial acetylation, C-H and amide III bands between $1445\text{--}1402.73\text{ cm}^{-1}$, and a prominent C-O-C/C-O stretch at 1083.46 cm^{-1} consistent with glycosidic linkages.

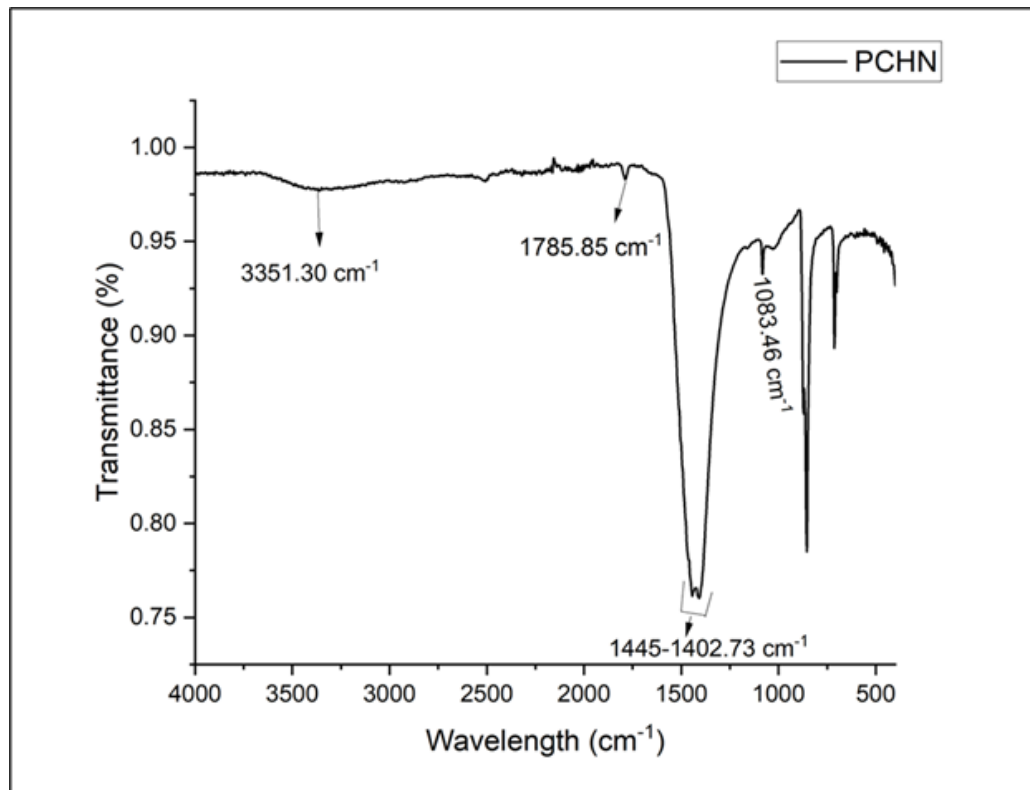


Figure 1: FT-IR spectrum of Periwinkle Chitosan sample (PCHN)

X-ray diffraction (XRD) of Periwinkle chitosan (PCHN)

The XRD pattern of the periwinkle chitosan (PCHN) (Figure 2) shows several sharp peaks between 20-45°, with a dominant reflection at ~30°, indicating a higher crystallinity than typically observed in native chitosan. These additional and more intense peaks suggest structural modification or phase incorporation, reflecting enhanced ordered domains and properties beyond those of standard semi-crystalline chitosan.

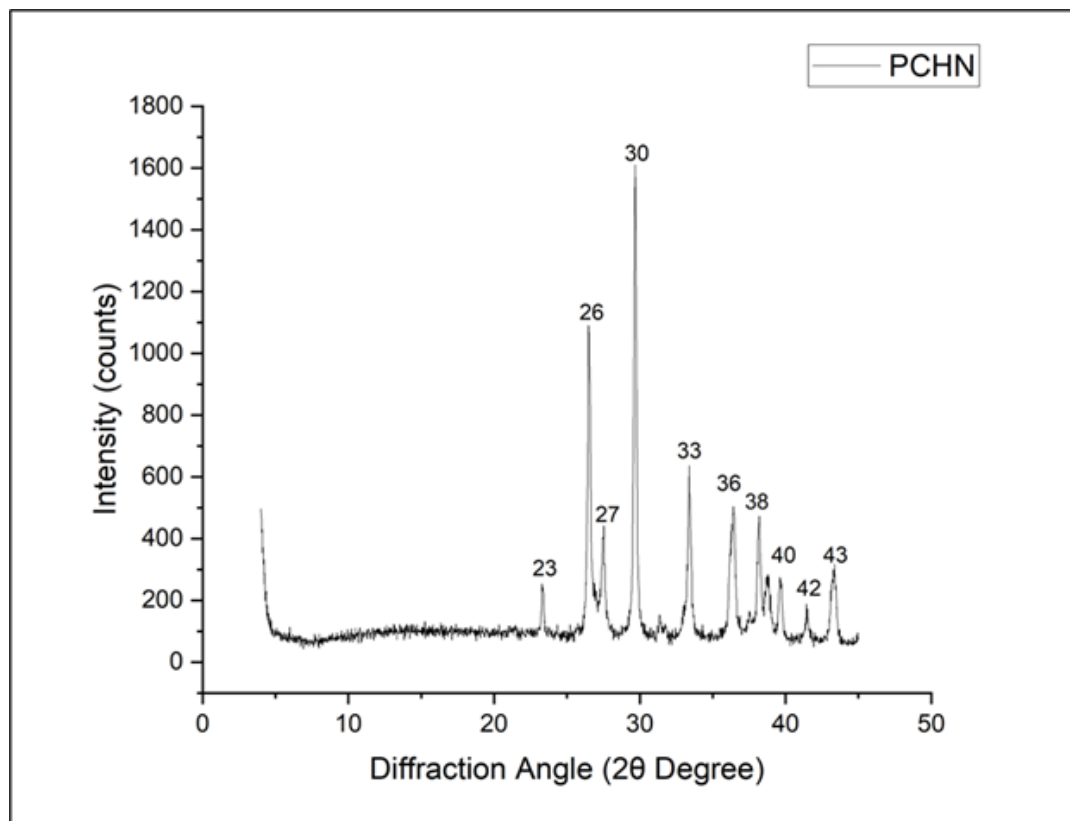


Figure 2: X-ray diffraction (XRD) of Periwinkle chitosan (PCHN)

SEM analysis of Periwinkle chitosan sample (PCHN)

Figure 3 shows that the periwinkle chitosan (PCHN) possesses a highly rough, porous, and flaky surface, with aggregated particles that become finer and more textured at higher magnifications. This morphology, typical of chitosan, indicates a large surface area, supporting its suitability for applications requiring strong adsorption, interaction, or bioactivity.

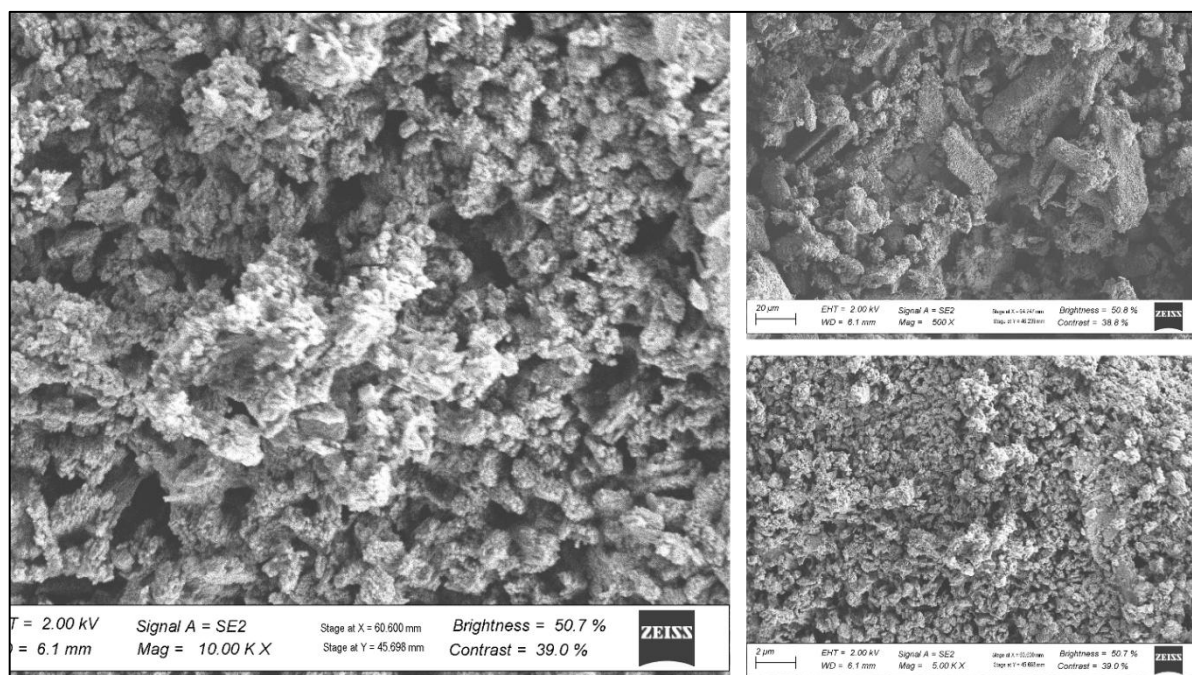


Figure 3: SEM analysis of Periwinkle chitosan sample (PCHN)

Energy-Dispersive X-ray Spectroscopy (EDX) analysis of chitosan extracted from periwinkle (PCHN)

Figure 4 shows the EDX analysis of periwinkle-extracted chitosan (PCHN), revealing prominent peaks for Calcium, Oxygen, and Carbon, with calcium being most abundant. The elevated calcium and oxygen levels indicate residual inorganic material, such as calcium carbonate, reflecting partial demineralisation during extraction, while the carbon content confirms the biopolymeric nature of chitosan.

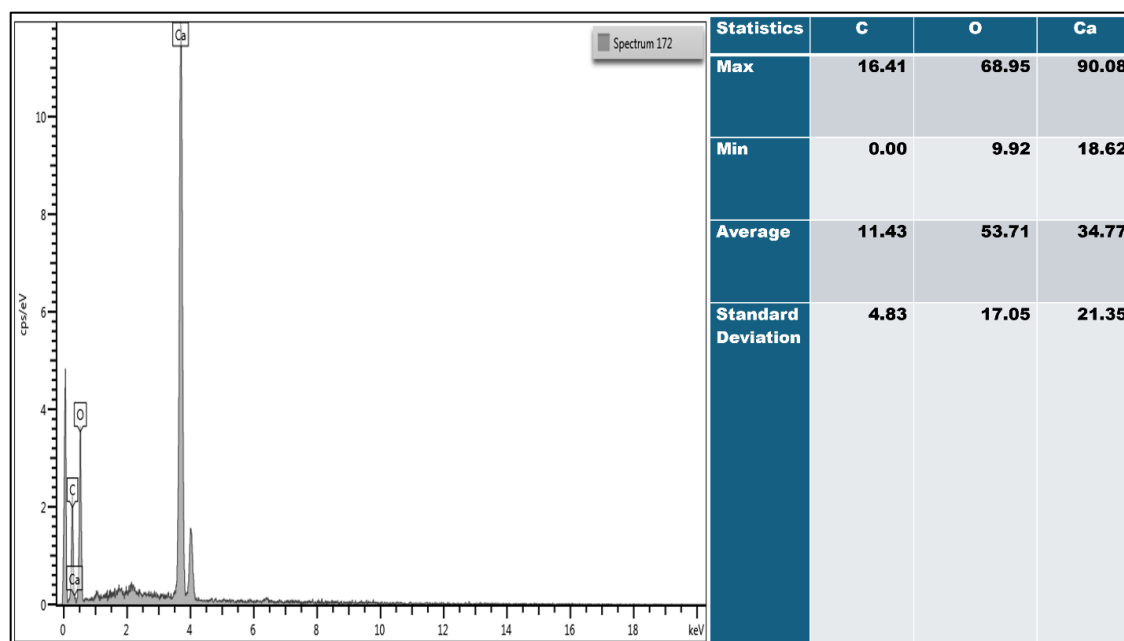


Figure 4: Energy-Dispersive X-ray Spectroscopy (EDX) analysis of chitosan extracted from periwinkle (PCHN).

Discussion

Physicochemical Parameters of the Chitosan Extracted from Periwinkle Shells

Chitosan was successfully extracted from periwinkle shells, as validated through a series of analytical methods. The extracted chitosan exhibited a degree of deacetylation of 86% (Table 1), closely aligning with values reported in existing literature. For example, Sánchez-Machado et al. (2024) documented a deacetylation degree of $98.69 \pm 0.45\%$ for chitosan derived from shrimp, highlighting the successful transformation of chitin into chitosan. Noteworthy properties of the extracted chitosan include its exceptionally low moisture content (0.5%) and protein content (0.4%) (Table 1), which are significantly lower than the values reported by Olaosebikan et al. (2021). These low levels suggest enhanced storage stability, making the material highly suitable for use in food and biomedical fields. Although the ash content measured at 5.6% exceeds the ideal threshold of $<2\%$, it remains comparable to the 12.78% ash content found in golden periwinkle shell chitosan. This elevated value may be attributed to partial demineralisation, as supported by residual elemental traces observed in the EDX analysis (Figure 9) (Ayu et al., 2023).

FT-IR spectrum of Periwinkle Chitosan sample (PCHN)

The FTIR spectrum of the sample labelled PCHN in Figure 1 shows several characteristic absorption peaks that provide insight into its chemical structure and functional groups. The broad absorption band at 3351.30 cm^{-1} is indicative of O-H and N-H stretching vibrations, typical of hydroxyl and amine groups found in chitosan or polysaccharide-based matrices. This confirms the hydrophilic nature of the material and the presence of hydrogen bonding, which is a common feature in natural biopolymers (Pati et al., 2021; Jáuregui-Nongrados et al., 2023; Ali et al., 2024).

The strong peak at 1785.85 cm^{-1} is characteristic of C=O stretching vibrations, typically associated with ester or carboxylic acid groups, and may suggest partial acetylation (Priscila et al., 2016). In the region $1445\text{--}1402.73\text{ cm}^{-1}$, bands commonly attributed to C-H bending vibrations and possibly amide III bands were observed. These confirm the polysaccharide backbone and secondary amide functionalities (Negrea et al., 2015; Ali et al., 2024). The distinct absorption at 1083.46 cm^{-1} corresponds to C-O-C and C-O stretching vibrations, typical of the glycosidic linkages in polysaccharides such as chitosan and cellulose (V. Gokula, 2018; Ali et al., 2024).

X-ray diffraction (XRD) of Periwinkle chitosan (PCHN)

The attached X-ray diffraction (XRD) pattern of the chitosan-based material (PCHN) as shown in Figure 2 displays multiple sharp peaks in the range of $2\theta = 20\text{--}45^\circ$, with the most intense peak observed at approximately 30° , and other discernible peaks at 23° , 26° , 27° , 33° , 36° , 38° , 40° , 42° , and 43° . This pattern indicates a high degree of crystallinity for the sample, as evidenced by the presence of intense, well-defined peaks over a lower amorphous background. In contrast, pure chitosan typically shows a broad peak around $2\theta = 19^\circ\text{--}20^\circ$ and a weaker peak near 10° , attributed to a largely amorphous structure with limited crystalline domains (Mahmoud et al., 2023; Hajer Ashour Abusnina et al., 2025). Literature reports confirm that chitosan's strong, broad peak at approximately 20° is characteristic of its semi-crystalline nature, with sharper or additional peaks often arising from composite formation or specific chemical modifications (Mahmoud et al., 2023). The presence of a major peak at 30° and additional peaks at higher angles in your sample suggests structural changes and increased crystallinity, likely due to functionalization or incorporation of other phases, which is above that of native chitosan and aligns with findings for chitosan-based hybrid materials or nanocomposites (Varma et al., 2021; Zaki et al., 2022). These structural differences may confer enhanced mechanical properties, stability, or functionality compared with unmodified chitosan, showing that your material exhibits both crystalline order and possible phase contributions not typically observed in pristine chitosan (Mahmoud et al., 2023; Varma et al., 2021).

SEM analysis of Periwinkle chitosan sample (PCHN)

The SEM images of the periwinkle chitosan sample (PCHN) in Figure 3 show a very rough and porous surface made up of many small, irregular particles clustered together. At lower magnification (500X), larger particle aggregates and a porous structure are visible. At higher

magnifications (5,000X and 10,000X), these aggregates break down into finer, flaky particles, creating a highly textured surface with many tiny gaps and voids. This porous, rough morphology is typical of chitosan materials prepared, which results in increased surface area (Song et al., 2022; Ahmed et al., 2025). Current literature reports chitosan having similar aggregated, flaky and porous structures, which enhance its properties for applications like wound healing, drug delivery, and environmental cleanup because the large surface area improves interaction with other substances (Mawazi et al., 2024). Thus, the observed microstructure of the PCHN sample aligns well with common findings about chitosan in scientific studies, confirming its potential usefulness where high surface area and porosity are important.

Energy-Dispersive X-ray Spectroscopy (EDX) analysis of chitosan extracted from periwinkle (PCHN)

The attached EDX (Energy-Dispersive X-ray Spectroscopy) results for chitosan extracted from periwinkle (Figure 4) reveal key details of its elemental composition. The spectrum graph indicates prominent peaks for Calcium (Ca), Oxygen (O), and Carbon (C), with Calcium showing the highest intensity peak. The corresponding table provides quantitative statistics with the average atomic concentration of Carbon being approximately 11.43%, Oxygen is 53.71%, and Calcium is 34.77%. The minimum and maximum values show that calcium ranges widely from 18.62% to 90.08%, while oxygen fluctuates between 9.92% and 68.95%, and carbon from 0% to 16.41%. The standard deviations denote variability in these elemental contents across the sample.

The high oxygen and calcium content is indicative of residual inorganic materials like calcium carbonate (CaCO_3), often found in shellfish exoskeletons such as periwinkle shells (Tertseghe et al., 2024). Chitosan itself is a biopolymer primarily composed of carbon, oxygen, and nitrogen, derived from the deacetylation of chitin. The relatively low carbon percentage here may be partly due to residual inorganic minerals, reflecting incomplete purification or retention of shell components in the extracted chitosan (Jiménez-Gómez & Cecilia, 2020). Literature on chitosan extracted from crustacean shells commonly reports calcium carbonate as a major contaminant that must be removed during purification to improve chitosan purity (Ayu et al., 2023). Compared to current literature, the elevated calcium level here suggests that the extraction process may not have fully demineralised the periwinkle shell material (Ayu et al., 2023). Additional purification could reduce calcium and enhance chitosan purity, aligning the sample more closely with standardized chitosan profiles reported in scientific studies.

References

1. Ahmed, H. A., El-Maradny, Y. A., Shalaby, M. A., El-Menshawly, H., & Abd EL-Wahab, A. E. (2025). Isolation and characterization of Chitosan from shrimp shell waste and the sustainable preparation of salicylic acid-loaded Chitosan nanoparticles for antibiofilm applications. *Scientific Reports*, 15(1). <https://doi.org/10.1038/s41598-025-03355-3>
2. Ali, A., Zahid, N., Manickam, S., Siddiqui, Y., Alderson, P. G., & Maqbool, M. (2013). Effectiveness of submicron chitosan dispersions in controlling anthracnose and maintaining quality of dragon fruit. *Postharvest Biology and Technology*, 86, 147–153. <https://doi.org/10.1016/j.postharvbio.2013.06.027>
3. Ali, S. A., Ali, E. S., Hamdy, G., Badawy, M. S. E. M., Ismail, A. R., El-Sabbagh, I. A., El-Fass, M. M., & Elsayy, M. A. (2024). Enhancing physical characteristics and antibacterial efficacy of chitosan through investigation of microwave-assisted chemically formulated chitosan-coated ZnO and chitosan/ZnO physical composite. *Scientific Reports*, 14(1), 9348. <https://doi.org/10.1038/s41598-024-58862-6>
4. Al-Manhel, A. J., Al-Hilphy, A. R. S., & Niamah, A. K. (2016). Extraction of chitosan, characterisation and its use for water purification. *Journal of the Saudi Society of Agricultural Sciences*.

5. Ayu, L. S., Rosida, D. F., Jariyah, Kongpichitchoke, T., Priyanto, A. D., & Putra, A. Y. T. (2023). Physicochemical Properties of Golden Apple Snail (*Pomacea canaliculata*) Shell Chitosan. *Food Science and Technology Journal (Foodscitech)*, 51-60. <https://doi.org/10.25139/fst.vi.5952>
6. Chaudhary, S., Kumar, S., Kumar, V., & Sharma, R. (2020). Chitosan nanoemulsions as advanced edible coatings for fruits and vegetables: Composition, fabrication and developments in last decade. *International Journal of Biological Macromolecules*, 152, 154-170. <https://doi.org/10.1016/j.ijbiomac.2020.02.276>
7. Ehrlich, H., Bazhenov, V. V., Debitus, C., de Voogd, N., Galli, R., Tsurkan, M. V., Wysokowski, M., Meissner, H., Bulut, E., Kaya, M., & Jesionowski, T. (2017). Isolation and identification of chitin from heavy mineralized skeleton of *Suberea clavata* (Verongida: Demospongiae: Porifera) marine demosponge. *International Journal of Biological Macromolecules*. <https://doi.org/10.1016/j.ijbiomac.2017.01.141>
8. Farajzadeh, F., Motamedzadegan, A., Shahidi, S.-A., & Hamzeh, S. (2016). The effect of chitosan–gelatin coating on the quality of shrimp (*Litopenaeus vannamei*) under refrigerated condition. *Food Control*, 67, 163-170. <https://doi.org/10.1016/j.foodcont.2016.02.040>
9. Hajer Ashour Abusnina, Nasser AAR El-Ghamaz, & Eman Asaad Gamal. (2025). AC electrical properties, thermal analysis and emission spectrum of Chitosan polymer. *Scientific Journal for Damietta Faculty of Science/Scientific Journal for Damietta Faculty of Science* , 0(0). <https://doi.org/10.21608/sjdfs.2025.352442.1211>
10. Hamdi, M., Hammami, A., Hajji, S., Jridi, M., Nasri, M., & Nasri, R. (2017). Chitin extraction from blue crab (*Portunus segnis*) and shrimp (*Penaeus kerathurus*) shells using digestive alkaline proteases from *P. segnis* viscera. *International Journal of Biological Macromolecules*, 101, 455–463. <https://doi.org/10.1016/j.ijbiomac.2017.02.103>
11. Hamed, I., Özogul, F., & Regenstein, J. M. (2016). Industrial applications of crustacean by-products (chitin, chitosan, and chitooligosaccharides): A review. *Trends in Food Science & Technology*, 48, 40-50. <https://doi.org/10.1016/j.tifs.2015.11.007>
12. Jáuregui-Nongrados, J., Alvarado, A. T., Mucha, M., Muñoz, A. M., Chávez, H., Molina-Cabrera, A., Cuba-García, P. A., Melgar-Merino, E. J., Bolarte-Arteaga, M., & Mori-Castro, J. A. (2023). Bioadsorption of silver ions by calcareous chitin, chitin and chitosan. *Journal of Pharmacy & Pharmacognosy Research*, 11(1), 101-109. https://doi.org/10.56499/jppres22.1529_11.1.101
13. Jiménez-Gómez, C. P., & Cecilia, J. A. (2020). Chitosan: A Natural Biopolymer with a Wide and Varied Range of Applications. *Molecules*, 25(17), 3981. <https://doi.org/10.3390/molecules25173981>
14. Katiyar, D., Hemantaranjan, A., & Singh, B. (2015). Chitosan as a promising natural compound to enhance potential physiological responses in plant: a review. *Indian Journal of Plant Physiology*, 20(1), 1-9. <https://doi.org/10.1007/s40502-015-0139-6>
15. Khatri, D., Panigrahi, J., Prajapati, A., & Bariya, H. (2020). Attributes of Aloe vera gel and chitosan treatments on the quality and biochemical traits of post-harvest tomatoes. *Scientia Horticulturae*, 259, 108837. <https://doi.org/10.1016/j.scienta.2019.108837>
16. Mahmoud, Z. H., Hamrouni, A., Kareem, A. B., Mostafa, M. A., Jalil alhakim, Z., & Majeed, A. H. (2023). Synthesis and characterization of chitosan sheet modified by varied weight ratio of anatase (TiO₂) nano mixture with Cr(VI) adsorbing. *Kuwait Journal of Science*, 50(3), 290-299. <https://doi.org/10.1016/j.kjs.2023.05.006>
17. Maqbool, M., Ali, A., & Alderson, P. G. (2010). A combination of gum arabic and chitosan can control anthracnose caused by *Colletotrichum musae* and enhance the shelf-life of banana fruit.

- Journal of Horticultural Science & Biotechnology, 85(5), 432–436. <https://doi.org/10.1080/14620316.2010.11512693>
18. Mawazi, S. M., Kumar, M., Ahmad, N., Ge, Y., & Mahmood, S. (2024). Recent Applications of Chitosan and Its Derivatives in Antibacterial, Anticancer, Wound Healing, and Tissue Engineering Fields. *Polymers*, 16(10), 1351. <https://doi.org/10.3390/polym16101351>
 19. Negrea, P., Caunii, A., Sarac, I., & Butnariu, M. (2015). The study of infrared spectrum of chitin and chitosan extract as potential sources of biomass. *Digest Journal of Nanomaterials and Biostructures*, 10(4), 1129-1138.
 20. Olaosebikan, A. O., Kehinde, O. A., Tolulase, O. A., & Victor, E. B. (2021). Extraction and characterization of chitin and chitosan from *Callinectes amnicola* and *Penaeus notialis* shell wastes. *Journal of Chemical Engineering and Materials Science*, 12(1), 1–30. <https://doi.org/10.5897/jcems2020.0353>
 21. Pati, S., Sarkar, T., Sheikh, H. I., Bharadwaj, K. K., Mohapatra, P. K., Chatterji, A., Dash, B. P., Edinur, H. A., & Nelson, B. R. (2021). γ -Irradiated Chitosan From *Carcinoscorpius rotundicauda* (Latreille, 1802) Improves the Shelf Life of Refrigerated Aquatic Products. *Frontiers in Marine Science*, 8. <https://doi.org/10.3389/fmars.2021.664961>
 22. Petrenko, I., Bazhenov, V. V., Galli, R., Wysokowski, M., Fromont, J., Schupp, P. J., Stelling, A. L., Niederschlag, E., Stöker, H., Kutsova, V. Z., Jesionowski, T., & Ehrlich, H. (2017). Chitin of poriferan origin and the bioelectrometallurgy of copper/copper oxide. *International Journal of Biological Macromolecules*. <https://doi.org/10.1016/j.ijbiomac.2017.01.084>
 23. Pichyangkura, R., & Chadchawan, S. (2015). Biostimulant activity of chitosan in horticulture. *Scientia Horticulturae*, 196, 49-65. <https://doi.org/10.1016/j.scienta.2015.09.031>
 24. Pornpienpakdee, P., Singhasurasak, R., Chaiyasap, P., Pichyangkura, R., Bunjongrat, R., Chadchawan, S., & Limpanavech, P. (2010). Improving the micropropagation efficiency of hybrid *Dendrobium* orchids with chitosan. *Scientia Horticulturae*, 124(4), 490-499. <https://doi.org/10.1016/j.scienta.2010.02.008>
 25. Priscila, F. P. B., Pablo, P. de M., Ccedil a, R ocirc mulo, D. A. A., Ana, C. R. A., Andr eacute a, R. C., & Fabiano, G. atilde es S. (2016). Efficacy of chitosan supported organic acaricide extract from *Melia azedarach* leaves on *Rhipicephalus (Boophilus) microplus* ticks. *African Journal of Biotechnology*, 15(26), 1391-1400. <https://doi.org/10.5897/ajb2016.15248>
 26. Ramasamy, P., Subhapradha, N., Thinesh, T., Selvin, J., Selvan, K. M., Shanmugam, V., & Shanmugam, A. (2017). Characterization of bioactive chitosan and sulfated chitosan from *Doryteuthis singhalensis* (Ortmann, 1891). *International Journal of Biological Macromolecules*, 99, 682-691. <https://doi.org/10.1016/j.ijbiomac.2017.03.041>
 27. Rasti, H., Parivar, K., Baharara, J., Iranshahi, M., & Namvar, F. (2017). Chitin from the mollusc *Chiton*: Extraction, characterization and chitosan preparation. *Iranian Journal of Pharmaceutical Research*, 16(1), 366-379.
 28. Sánchez-Machado, D. I., López-Cervantes, J., Escárcega-Galaz, A. A., Campas-Baypoli, O. N., Martínez-Ibarra, D. M., & Rascón-León, S. (2024). Measurement of the degree of deacetylation in chitosan films by FTIR, ¹H NMR and UV spectrophotometry. *MethodsX*, 12, 102583-102583. <https://doi.org/10.1016/j.mex.2024.102583>
 29. Song, W., Zhang, Q., Guan, Y., Li, W., Xie, S., Tong, J., Li, M., & Ren, L. (2022). Synthesis and Characterization of Porous Chitosan/Saccharomycetes Adsorption Microspheres. *Polymers*, 14(11), 2292-2292. <https://doi.org/10.3390/polym14112292>
 30. Tertsegha, S., Akubor, P. I., Iordekighir, A. A., Christopher, K., & Okike, O. O. (2024). Extraction and Characterization of Chitosan from Snail Shells (*Achatina fulica*). *Journal of Food Quality and Hazards Control*, 11. <https://doi.org/10.18502/jfqhc.11.3.16590>

31. Usman, A., Zia, K. M., Zuber, M., Tabasum, S., Rehman, S., & Zia, F. (2016). Chitin and chitosan based polyurethanes: A review of recent advances and prospective biomedical applications. *International Journal of Biological Macromolecules*, 86, 630-645. <https://doi.org/10.1016/j.ijbiomac.2016.02.004>
32. V. Gokula, V. (2018). Extraction and FTIR characterization of chitosan from *Portunus pelagicus* shell wastes. *International Journal of Advanced Scientific Research and Management*, 3(10). <https://doi.org/10.36282/ijasrm/3.10.2018.879>
33. Varma, R., Vasudevan, S., Chelladurai, S., & Narayanasamy, A. (2021). Synthesis and Physicochemical Characteristics of Chitosan Extracted from *Pinna deltoides*. *Letters in Applied NanoBioScience*, 11(4), 4061-4070. <https://doi.org/10.33263/lianbs114.40614070>
34. Zaki, A. A., Khalafalla, M., Alharbi, K. H., & Khalil, K. D. (2022). Synthesis, characterization and optical properties of chitosan–La₂O₃ nanocomposite. *Bulletin of Materials Science*, 45(3). <https://doi.org/10.1007/s12034-022-02697-2>